The NLRP3 Activation in Infiltrating Macrophages Contributes to Corneal Fibrosis by Inducing TGF-β1 Expression in the Corneal Epithelium

Jing Xu,[1] Peng Chen,[1] Xiaoyu Luan,[1] Xinying Yuan,[1] Susu Wei,[1] Yaxin Li,[1] Chuanlong Guo,[2] Xianggen Wu,[2] and Guohu Di[1]

[1]School of Basic Medicine, Medical College, Qingdao University, Qingdao, China
[2]College of Chemical Engineering, Qingdao University of Science and Technology, Qingdao, China

Correspondence: Guohu Di, Qingdao University, 308 Ningxia Road, Qingdao 266071, China; diguohu@qdu.edu.cn.

JX and PC contributed equally.

Received: March 29, 2022
Accepted: June 27, 2022
Published: July 15, 2022

Citation: Xu J, Chen P, Luan X, et al. The NLRP3 activation in infiltrating macrophages contributes to corneal fibrosis by inducing TGF-β1 expression in the corneal epithelium. *Invest Ophthalmol Vis Sci.* 2022;63(8):15. https://doi.org/10.1167/iovs.63.8.15

Purpose. To explore the effect and mechanism of NOD-, LRR-, and pyrin domain-containing protein 3 (NLRP3) inflammasomes on corneal fibrosis.

Methods. The wild-type, *NLRP3* knockout (KO), and myeloid cell-specific *NLRP3* KO (*NLRP3* Lyz-KO) C57 mice were used to establish a corneal scarring model. NLRP3 inhibitor, IL-1β neutralizing antibody, and an IL-1R antagonist were used to investigate the role of NLRP3 and IL-1β in corneal fibrosis. The expression of the NLRP3 signaling pathway related proteins, alpha-smooth muscle actin, TGF-β was determined by quantitative real-time polymerase chain reaction, Western blotting, and immunofluorescence staining. Flow cytometry was used to detect the infiltration of macrophages during corneal fibrosis.

Results. The components of the NLRP3 inflammasomes were elevated and activated during corneal scarring. Additionally, genetic or chemical-mediated blocking of NLRP3 as well as IL-1β significantly alleviated corneal fibrosis. Moreover, neutrophil ($CD45^+Ly6G^+$) and macrophage ($CD45^+$ $F4/80^+$) accumulation increased in the cornea during the progression of corneal fibrosis. Intriguingly, the increased concentrations of NLRP3 and IL-1β were prominently colocalized with the infiltrating $F4/80^+$ macrophages. Expectedly, NLRP3 Lyz-KO mice exhibited a marked decrease in their corneal fibrosis symptoms. Mechanistically, the activation of IL-1β or macrophage NLRP3 stimulated the expression of TGF-β1 in the corneal epithelial cells, whereas an NLRP3 deficiency decreased its expression in the corneal epithelium.

Conclusions. These observations revealed that the NLRP3 inflammasome activation in infiltrating macrophages contributes to corneal fibrosis by regulating corneal epithelial TGF-β1 expression. Targeting the NLRP3 inflammasome might be a promising strategy for the treatment of corneal scarring.

Keywords: NLRP3, knockout, macrophages, corneal fibrosis, TGF-β1

Ocular surface diseases, such as corneal scarring (or fibrosis), occur owing to trauma, infection, or surgical intervention, thereby compromising corneal transparency and causing visual impairment.[1,2] The disruption of corneal transparency blocks the transmission of external light to the retina, which is essential for optimal visual acuity. Corneal tissue repair is a dynamic process involving three phases, namely, the initial inflammatory phase, the intermediate proliferative phase, and the ultimate remodeling phase.[3–5] Various inflammatory cells secrete cytokines that activate corneal stromal cells that, in turn, cause excessive connective tissue proliferation and scar formation.[4] During this inflammatory phase, corneal epithelial cells release cytokines and mediators that trigger an inflammatory response by recruiting neutrophils, macrophages, and other inflammatory cells. In the remodeling phase, the damaged corneal epithelial cells as well as infiltrating inflammatory cells secrete large amounts of cytokines, such as stromal cell-derived factor-1, TGF-β1, and platelet-derived growth factor.[6] These can transform the corneal stromal cells into alpha-smooth muscle actin (α-SMA)–positive myofibroblasts that synthesize and release collagen, fibronectin, hyaluronic acid, and other extracellular matrix components.[7,8]

Macrophages are essential for the regulation of fibroblast functions during the repair of corneal injuries.[9] Specifically, during the proliferative phase, myofibroblasts are surrounded by massive macrophages. In fact, these two types of cells remain in close spatial contact and interact with each other to mediate corneal stromal remodeling and fibrosis.[10,11] Furthermore, the cytokine secretion by macrophages is also vital for the repair of corneal injuries. In fact, during the inflammatory phase, activated M1 macrophages migrate to the periwound area. After activation, the macrophages not only engulf and remove foreign bodies, pathogens, and cellular debris, but also secrete multiple inflammatory factors, including IL-1, IL-6, TNF-α, and other cytokines.[11,12]

These inflammatory factors, in turn, cause the further accumulation of macrophages at the injury site. After removing the cellular debris, the macrophages transform into an anti-inflammatory phenotype (M2) and secrete anti-inflammatory factors, such as IL-10 and IL-4, to promote inflammatory regression and epithelial repair.[13]

The NOD-, LRR-, and pyrin domain-containing protein 3 (NLRP3) is an important member of the Nod-like receptor family of pattern recognition receptors. Interestingly, NLRP3, an essential component of intrinsic immunity, plays a key role in mediating the functions of macrophages during the body's immune responses.[14] When a signal stimulus is generated, NLRP3 recognizes the corresponding signal and undergoes oligomerization as well as metamorphosis to recruit the apoptosis-associated speck-like protein containing a CARD (ASC) and pro-caspase 1, and they form the NLRP3–ASC–pro-caspase 1 inflammatory complex. Coincidentally, the NLRP3/IL-1β pathway is activated in macrophages in some large organs, such as lung, kidney, and liver, during the development of tissue fibrosis.[15–17] Moreover, recent studies have reported that IL-1β induces apoptosis of corneal stromal cells and participates in the repair of corneal injuries, as well as in corneal neovascularization.[18,19] However, the involvement of the NLRP3/IL-1β pathway of macrophages in corneal stromal cell activation and corneal scar formation is yet to be confirmed.

This study determined the critical role of NLRP3/IL-1β signaling pathway in the corneal myofibroblast differentiation and corneal scar formation. Simultaneously, it was observed that blockade of the NLRP3/IL-1β pathway promoted the maintenance of corneal transparency. Mechanistically, activation of the NLRP3 inflammasome releases IL-1β, which stimulates TGF-β1 synthesis in corneal epithelial cells. Moreover, this increased TGF-β1 synthesis induces a corresponding increase in the differentiation of myofibroblasts. Therefore, our observations provide some fundamental insights with respect to the molecular mechanisms involved in corneal scarring or fibrosis that, in turn, might help to develop novel therapeutic strategies for these conditions in future.

Methods

Animals

All animal experiments strictly conformed with the ARVO Statement for the Use of Animals in Ophthalmic and Vision Research, and the entire study design was formally approved by the Ethics Committee Medical College of Qingdao University (QDU-AEC-2021192). Wild-type (WT), male, 8 to 10 weeks old, C57BL/6 mice were purchased from Ji'nan Pengyue Experimental Animal-Breeding Co. Ltd. (Ji'nan, Shandong, China). Additionally, B6.129P2-Lyz2tm101(Cre)/V (*Lyz-Cre*) mice were purchased from Viewsolid Biotech Co. Ltd. (Beijing, China). B6.C-Tg(CMV-cre)/Nju (*CMV-Cre*) and B6JNju;B6NNju-Nlrp3(flper)^{tm1}/Nju [*NLRP3* locus of X-over P1 (*NLRP3^{loxp}*)] mice (loxp sites flanking the entire *NLRP3* sequence) were purchased from GemPharmatech Co., Ltd. (Nanjing, China). To produce whole body deficiency of *NLRP3*, the *NLRP3^{loxp}* mice were crossbred with *CMV-Cre* mice to generate *CMV-Cre^{+}NLRP3$^{loxp/loxp}$* mice (*NLRP3$^{-/-}$*, *NLRP3* knockout [KO]). Furthermore, myeloid cell-specific *NLRP3* KO mice (*LyzCre^{+}NLRP3$^{loxp/loxp}$*, *NLRP3* Lyz-KO) were generated by crossing the *NLRP3^{loxp}* mice with *Lyz-Cre* mice. All breeds, except the WT mice, were backcrossed for at least 10 generations on a C57BL/6 background.

Corneal Scarring Model

The corneal scarring mice model was created according to previous reports[20,21] with minor modification. First, the mice were subjected to gaseous anesthesia (2% isoflurane in oxygen; VETEASY, RWD Life Science, Shenzhen, China), and 3-mm diameter corneal epithelium, as well as anterior stromal tissue of one eye were mechanically removed using Algerbrush II corneal rust ring remover (Alger Co, Lago Vista, TX). The other eye was used as a normal control. Subsequently, a topical ofloxacin eye ointment (Santen Pharmaceutical Co. Ltd., Tokyo, Japan) was applied to the injured eye. To assess corneal wound healing and determine the grade of corneal scarring, images of the eyes (normal control as well as injured) were captured on days 1, 3, 5, and 7 after injury, using a slit lamp (YZ5S; 66 Vision Tech Co, Ltd, Suchow, China), with or without 0.25% fluorescein sodium staining. The corneal scarring was graded on a scale of 0 to 4, where a grade of 0 meant completely clear, 0.5 meant minimal scarring with careful oblique illumination, 1 implied mild scarring not interfering with visibility of fine iris details, 2 meant mild opacification of iris details, 3 meant moderate opacification of the iris and lens, and 4 implied complete opacification of the anterior chamber and iris.[22] ImageJ software was used to analyze the fluorescein sodium stained area and, subsequently, the percentage or rate of wound healing was calculated. To determine the effects of NLRP3 and IL-1β on the development of corneal fibrosis, the model mice received subconjunctival injections of 5 µL NLRP3 inhibitor (MCC950, 10 mg/mL; MCE, Houston, TX), IL-1β neutralizing antibody (a-IL-1β antibody, 100 ng/mL; R & D Systems, Minneapolis, MN), IL-1R antagonist (anakinra, 10 mg/mL; MCE), or PBS (control) on days 0, 3, and 6 after injury. Thereafter, the mice were euthanized on day 7 after injury. Finally, the mouse eyeballs were collected for immunofluorescence staining, and the corneas were harvested for Western blot, quantitative RT-PCR (qRT-PCR), and flow cytometry analyses.

Isolation and Stimulation of Peritoneal Macrophages

The peritoneal macrophages were isolated, according to a previously described protocol.[23] First, the WT and *NLRP3$^{-/-}$* mice were humanely euthanized, followed by sterilization with 75% ethanol for 5 minutes. Thereafter, the peritoneal cavity was lavaged using 5 mL PBS supplemented with 0.1% EDTA to collect the macrophages. First, the cells were resuspended in 5 mL red blood cell lysis buffer for 2 minutes to lyse the erythrocytes. Thereafter, the cell suspension was centrifuged at 1000 rpm for 5 minutes and washed with PBS. Subsequently, the cells were resuspended in RPMI-1640 medium supplemented with 10% fetal bovine serum and 1% penicillin/streptomycin and plated in a six-well plate at 4×10^6 cells/well. After sedimentation, the medium was replaced with a fresh medium to discard unattached cells. Thereafter, to induce a proinflammatory response, the purified peritoneal macrophages were pretreated with 100 ng/mL lipopolysaccharide (LPS InvivoGen, Cayla, France) from *Escherichia coli* K12 for 3 hours, followed by the

Table. Gene-Specific Primers Used in the qPCR

Gene	Accession Number	Primer Sequences
m-GAPDH	NM_001289726.1	Forward: GCCACCCAGAAGACTGTGGAT Reverse: GGAAGGCCATGCCAGTGA
m-α-SMA	NM_007392.3	Forward: TGCCGAGCGTGAGATTGTC Reverse: CGTTCGTTTCCAATGGTGATC
m-Collagen I	NM_007742.4	Forward: TGACTGGAAGAGCGGAGAGTACT Reverse: TTCGGGCTGATGTACCAGTTC
m-Fibronectin	NM_010233.2	Forward: TCATTTCATGCCAACCAGTTG Reverse: AACCTCTTCCCGAACCTTGTG
m-NLRP3	NM_145827.4	Forward: AACCTCTTCCCGAACCTTGTG Reverse: AGGTTGCAGAGCAGGTGCTT
m-ASC	NM_023258.4	Forward: TGGACGCCATAGATCTCACTGA Reverse: CTGCCACAGCTCCAGACTCTT
m-Caspase1	NM_009807.2	Forward: CTGGGACCCTCAAGTTTTGC Reverse: CCCTCGGAGAAAGATGTTGAAA
m-IL-1β	NM_008361.4	Forward: CTTTCCCGTGGACCTTCCA Reverse: CTCGGAGCCTGTAGTGCAGTT
m-IL-18	NM_008360.2	Forward: GACCAAGTTCTCTTCGTTGACAAAA Reverse: CTATCCTTCACAGAGAGGGTCACA
m-TGF-β	NM_011577.2	Forward: CAACAATTCCTGGCGTTACCTT Reverse: CAAGAGCAGTGAGCGCTGAA
h-GAPDH	NM_002046.7	Forward: CATGTTCGTCATGGGTGTGAA Reverse: GGCATGGACTGTGGTCATGAG
h-TGF-β	NM_000660.7	Forward: CGCCAGAGTGGTTATCTTTTGA Reverse: CGGTAGTGAACCCGTTGATGT

addition of 10 µM nigericin (Nig; Sigma, St Louis, MO) for 1 hour. The macrophages were divided into four groups, namely, WT-unstimulated, WT-LPS + Nig, KO-Con, and KO-LPS + Nig. After stimulation, the cell supernatants were collected and prepared for ELISA, and the cells were harvested for Western blotting analysis.

Cell Culture

Human corneal epithelial cells were cultured as previously described.[24] In brief, human corneal epithelial cells were cultured in Dulbecco's modified Eagle's medium/F12 medium (DF12, Hyclone, Logan, UT) containing 10% fetal bovine serum (ExCell Bio, Shanghai, China) and 1% streptomycin/penicillin (Solarbio, Beijing, China) with 5% CO_2 at 37°C. When the cells reached 70% to 80% confluency, rhIL-1β (R & D Systems; 0, 1, 5, and 10 ng/mL) was added to the medium, followed by a 24-hour incubation period. Subsequently, the cell lysates were prepared for Western blotting and qRT-PCR analyses. Additionally, primary mouse corneal epithelial cells (pMCECs) were harvested from eyeballs of WT mice. First, the eyeballs were soaked in 1.2 U/mL Dispase II (Gibco, Waltham, MA) for 16 hours at 4°C. Thereafter, the corneal epithelium was separated and placed in a 24-well plate for adherent culture. The cells were maintained in keratinocyte serum-free medium (Gibco) supplemented with 2% serum-free culture factor B27 (ThermoFisher Scientific, Waltham, MA), 1% penicillin/streptomycin, 1% insulin-transferrin-selenium (Gibco), and 0.1% Y-27632 (Sigma) in an incubator containing 5% CO_2 at 37°C. The supernatant from the macrophages (WT-unstimulated, WT-LPS + NIG, KO-CON, and KO-LPS + NIG) was mixed with an equal volume of keratinocyte serum-free medium complete medium to form the conditioned medium for the pMCECs. After 24 hours of culture, the cells were finally collected for qRT-PCR analysis.

Quantitative Real-Time PCR

Total RNA was extracted from the corneal tissue (three corneas were pooled together as a sample) or cells using GeneJET RNA purification kit (ThermoFisher Scientific), according to the manufacturer's protocol. Subsequently, cDNAs for *α-SMA*, collagen I, fibronectin, *NLRP3*, *ASC*, caspase 1, *IL-1β*, and *IL-18* were synthesized using PrimeScript First Strand cDNA synthesis kit (TaKaRa, Dalian, China), as per the manufacturer's guidelines. As previously reported,[25] the cDNAs were subjected to qRT-PCR using SYBR Premix Ex Taq (Vazyme, Nanjing, China), and the reaction products were analyzed using Bio-Rad CFX96 Real-Time Systems (Bio-Rad, Hercules, CA), with glyceraldehyde 3-phosphate dehydrogenase (*GAPDH*) as an internal control. All primer sequences used for PCR analysis are specified in the Table.

Western Blot Analysis and ELISA

As previously described,[26] corneal tissues (three corneas per sample) and cells were subjected to radioimmunoprecipitation assay buffer lysis to extract the total protein. Thereafter, the protein samples were separated using 10% sodium dodecyl sulfate-polyacrylamide gel electrophoresis. The separated proteins were transferred to polyvinylidene fluoride membranes (Millipore, Billerica, MA). After blocking the membranes with 5% skim milk for 1 hour, they were incubated with primary antibodies against NLRP3 (1:1000; Adipogen Life Sciences, San Diego, CA), ASC (1:1000; Abcam), IL-1β (1:1000; Abcam), caspase 1 (1:1000; Abclonal, Wuhan, China), α-SMA (1:1000, Abcam), TGF-β1 (1:1000, Affinity Biosciences, Cincinnati, OH), and β-actin (1:1000, Affinity Biosciences). Subsequently, the membranes were incubated with the corresponding horseradish peroxidase-conjugated secondary antibodies (1:1000; Zhongshan Jinqiao Biotech, Beijing, China). Finally, the proteins were visualized using an automatic chemilumi-

Investigative Ophthalmology & Visual Science

nescence image analysis system (Tanon, Shanghai, China), and the expression levels of the target proteins were analyzed using ImageJ software with β-actin as an internal control. The IL-1β levels in the supernatants of the macrophage suspensions were analyzed using commercially available murine IL-1β ELISA kits (BOSTER, Pleasanton, CA), according to the manufacturer's instructions.

Flow Cytometry Analysis

As previously reported,[27] the corneal tissues (four corneas per group) were digested using RPMI media containing 0.05 mg/mL DNase I (Roche Corp., Indianapolis, IN) and 2 mg/mL collagenase type IV (Sigma-Aldrich Corp., St. Louis, MO) for 1 hour at 37°C to collect corneal monocyte. Thereafter, the digested mixture was filtered through a 70-µm cell strainer (Becton & Dickinson, Franklin Lakes, NJ) to obtain the cell suspension. The single cell suspensions were stained with FITC-conjugated anti-mouse CD45 (#103206, BioLegend, San Diego, CA), allophycocyanin-conjugated anti-mouse F4/80 (#123115, BioLegend), and phycoerythrin-conjugated anti-mouse Ly6G (#127608, BioLegend) for 30 minutes. Subsequently, the cells were washed twice with PBS and resuspended in the same. Finally, the cells were analyzed using LSR II flow cytometer (BD Biosciences Inc., San Jose, CA), and data were analyzed using FlowJo software vX.5.3 (FlowJo LLC., Ashland, OR).

Immunofluorescence Staining

For immunohistochemical analyses, cryosections of the mouse eyeball specimens were fixed in 4% paraformaldehyde and blocked using 5% BSA. The sections were incubated with primary antibodies, namely anti–α-SMA (1:100, Abcam), anti-NLRP3 (1:100, Abcam), anti-IL-1β (1:100, Abcam), and anti–TGF-β1 (1:100, Affinity Biosciences) overnight at 4°C. Thereafter, the tissue sections were incubated with corresponding fluorescein-conjugated secondary antibodies. For double immunofluorescence labeling, the tissue sections were initially incubated with antibodies against NLRP3 or IL-1β, followed by fluorescein-conjugated secondary antibody and anti-F4/80 staining. Finally, the nuclei were stained using 4′,6-diamidino-2-phenylindole (DAPI; Beyotime, Shanghai, China) and examined using an Olympus BX50 fluorescence microscope (Tokyo, Japan).

Statistical Analyses

All data in this study were obtained from at least three independent experiments, and they are presented as mean ± standard deviation. Prism 8.0 software (GraphPad, San Diego, CA) was used to perform the statistical analyses. Differences between two groups were determined using an unpaired Student *t*-test, and the differences were considered as statistically significant if the *P* values was less than 0.05.

Results

Corneal Scarring Is Associated With NLRP3 Activation

During the progression of corneal fibrosis in the corneal scarring mice models, the injured corneas were photographed using a slit-lamp microscope, with or without fluorescein sodium staining, on days 0, 1, 3, 5, and 7 after injury. In the control group, there was a disk-shaped, central scar with a high scar grade (Figs. 1A, B). The corneal wound healed completely on day 7 after injury (Figs. 1A, C). Coincidentally, the qRT-PCR analysis of the corneal tissues revealed a remarkable increase in the expression levels of α-SMA, collagen I, and fibronectin mRNAs on day 5, and these high expression levels persisted on day 7 (Fig. 1D). Subsequently, the mRNA levels of the NLRP3 inflammasome components were examined to explore the inflammatory mechanism of corneal fibrosis. As shown in Figure 1E, the inflammasome activation led to an increased secretion of NLRP3, ASC, caspase 1, and downstream cytokines, like IL-1β and IL-18, in the corneal tissue. Moreover, there was a simultaneous increase in the expression levels of the proteins of the NLRP3 inflammasome as well as the fibrosis marker α-SMA (Figs. 1F, G). Therefore, these results indicate the close association of NLRP3 activation with the development of a corneal scar.

Inhibition of IL-1β Alleviates Corneal Fibrosis

To investigate the role of IL-1β in corneal fibrosis, the corneal fibrosis mice models were treated with a-IL-1β antibody and anakinra. As depicted in Figures 2A and B, blocking the IL-1β signaling pathway reversed corneal fibrosis in vivo. Additionally, it led to a marked improvement in the healing of corneal defects (Supplementary Fig. S1) on day 3 after injury. Furthermore, α-SMA–specific immunofluorescent staining revealed an apparent increase in the accumulation of myofibroblasts in the control group, whereas a-IL-1β antibody and anakinra treatments diminished their numbers (Fig. 2C). In fact, qRT-PCR revealed a decrease α-SMA, collagen I mRNA level in the corneas with a-IL-1β antibody and anakinra treatments (Fig. 2D). Furthermore, Western blotting analysis confirmed that the inhibition of IL-1β could decrease α-SMA protein expression in the corneal tissues (Fig. 2E).

Small Inhibitor MCC950 Inhibits Corneal Scarring

To explore the potential role of the NLRP3 inflammasome in the regulation of corneal scar formation, an NLRP3 inhibitor (MCC950) was subconjunctivally administered in vivo. After injury, the mice in the control group (PBS) developed remarkable corneal opacity, whereas the MCC950-pretreated mice exhibited a notably lesser corneal opacity than that in the control group; in fact, the latter portrayed a near-complete restoration of corneal transparency, especially on day 7 after injury (Figs. 3A, B). Moreover, the corneal epithelial was repaired without accelerated healing in the MCC950-pretreated mice (Supplementary Fig. S2). At 7 days after injury, corneal tissues were collected, and the effect of MCC950 on fibrosis was determined with respect to the mRNA and protein expression levels. The qRT-PCR analysis revealed a substantial decrease in the expressions of α-SMA and collagen I in the MCC950-treated corneas, as compared with that in the control group corneas (Fig. 3C). Moreover, immunostaining and Western blotting (Fig. 3D) confirmed that MCC950 significantly inhibited α-SMA expression in corneas.

KO of *NLRP3* Reduces Corneal Scarring

Because the inhibition of NLRP3 decreased corneal scarring, it was necessary to further investigate the

Investigative Ophthalmology & Visual Science

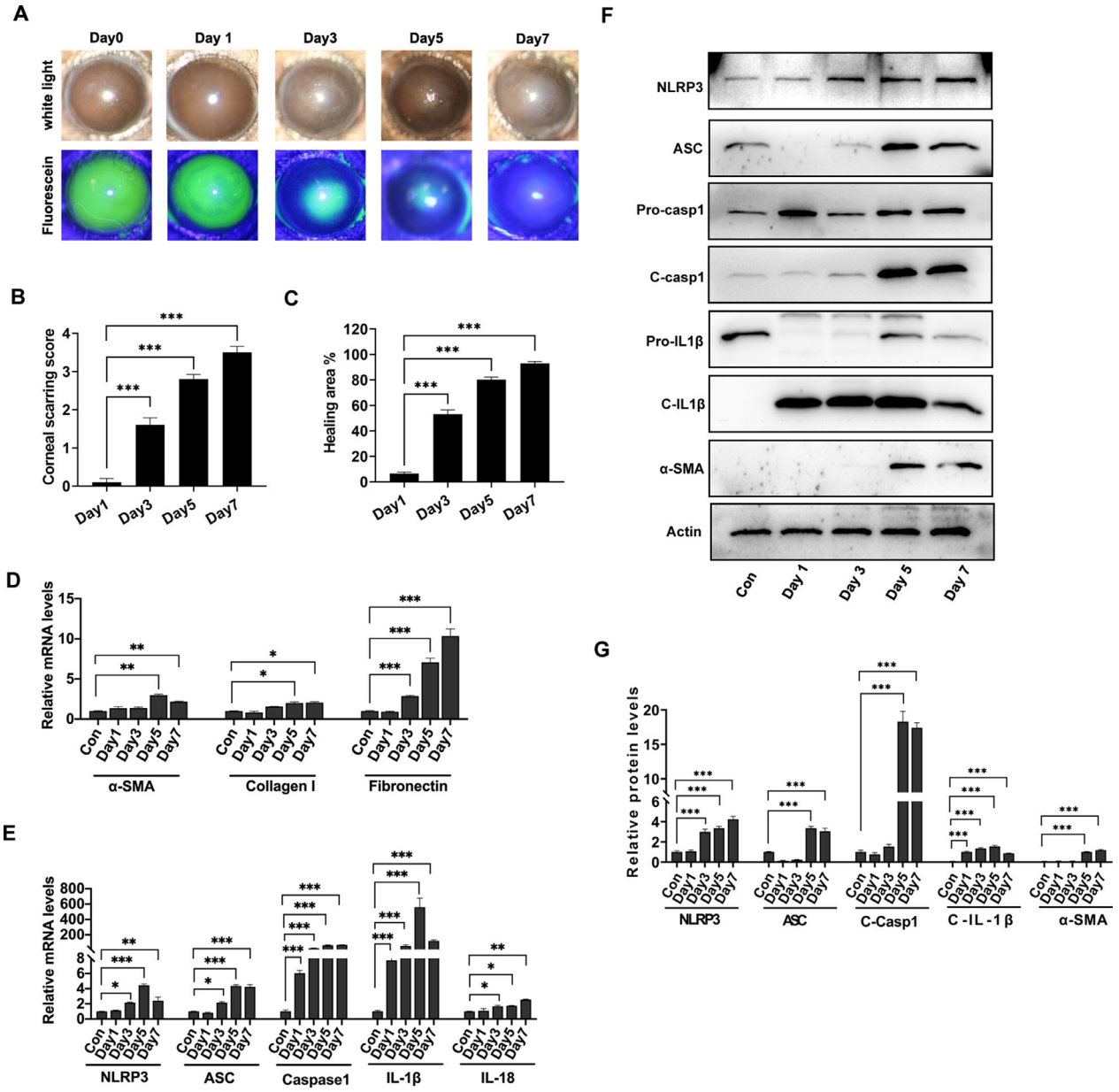

Figure 1. Corneal scarring is associated with the activation of the NLRP3. Corneal scarring model was established by mechanical-injury in WT mice. The corneas were gathered on days 1, 3, 5, and 7 after injury. (**A**, Representative images of injured cornea under bright-field microscopic (top) and corneal epithelial defect area with fluorescein sodium staining (bottom). (**B**, The quantification of corneal scarring (n = 10). (**C**, The quantification of corneal epithelial wound healing rate (n = 10). (**D**, The mRNA levels of fibrosis markers (α-SMA, collagen I, and fibronectin) in the corneal tissue of an established corneal scarring model. (**E**, The mRNA levels of NLRP3-associated inflammatory markers (NLRP3, ASC, caspase1, IL-1β, and IL-18) in the corneal tissue of an established corneal scarring model. (**F**, **G**) Western blot and statistical analysis for the protein expression of NLRP3, caspase1, ASC, pro-caspase1, c-caspase1, pro-IL-1β, c-IL-β, and α-SMA in corneas. All experiments were repeated three times independently. Data are presented as the mean ± standard deviation. *P < 0.05, **P < 0.01, ***P < 0.001. ASC, apoptosis-associated speck-like protein containing a CARD; c-caspase1, cleaved caspase 1; C-IL-β, cleaved IL-1 beta.

involvement of NLRP3 in corneal fibrosis using *NLRP3* KO mice. Coincidentally, in comparison with the WT mice, the *NLRP3*$^{-/-}$ mice experienced a reduced corneal scarring; that is, their corneal scars exhibited lower scar grades than that in the WT mice (Figs. 4A, B). Additionally, the NLRP3$^{-/-}$ mice had a better corneal epithelial wound healing ability than that in the WT mice (Supplementary Fig. S3), as observed on day 3 after injury. Moreover, qRT-PCR analysis revealed that the α-SMA and collagen I mRNAs were markedly decreased in the corneas of *NLRP3*$^{-/-}$ mice after injury (Fig. 4C). This finding was further confirmed by the weaker immunostaining (Fig. 4D) and a decreased protein expression of α-SMA (Fig. 4E) in the *NLRP3*$^{-/-}$ mice corneas, as compared with that in the WT mice corneas on day 7 after injury. These observations indicate that inhibition of the NLRP3 signaling pathway reverses corneal scarring in vivo.

Investigative Ophthalmology & Visual Science

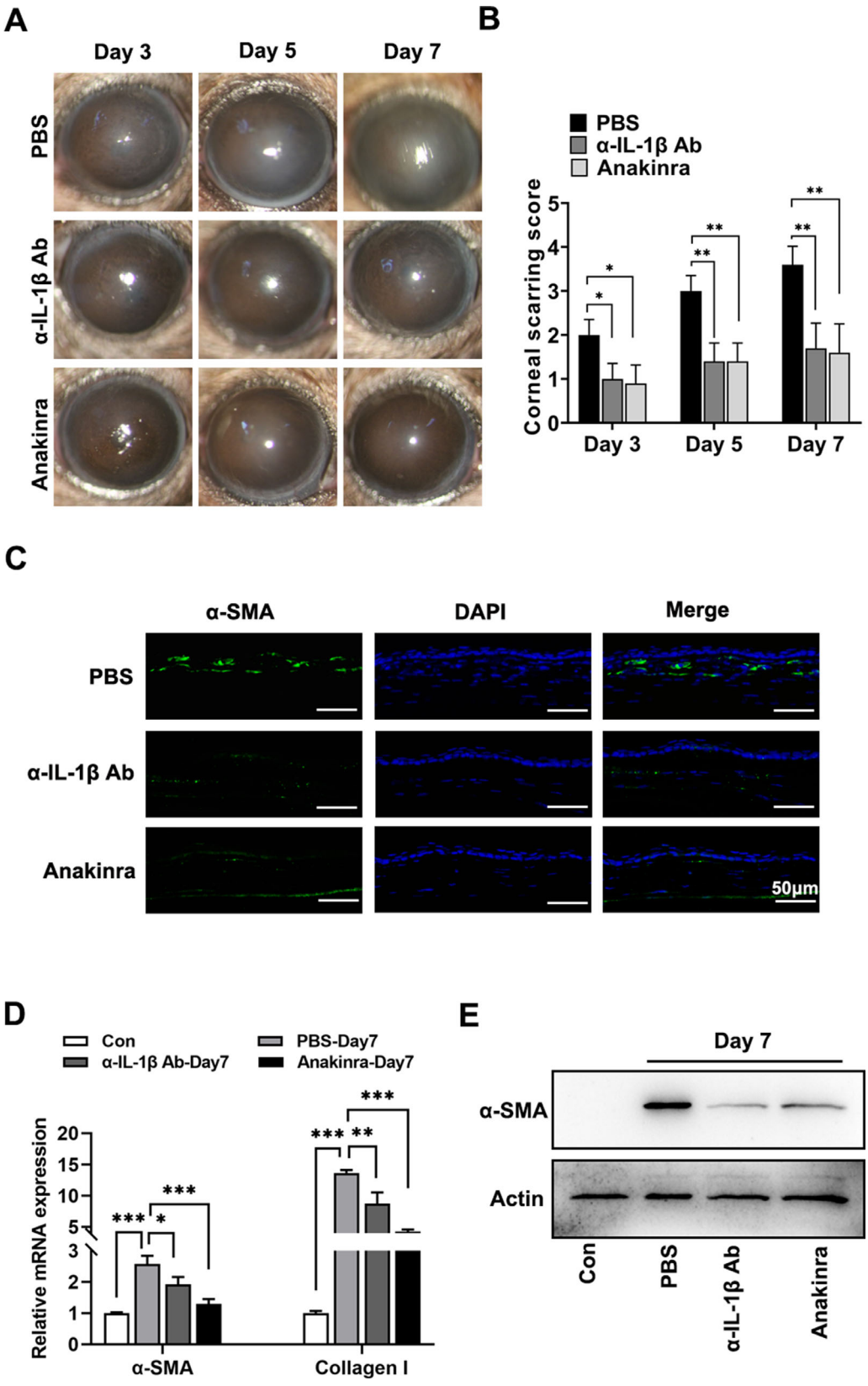

Figure 2. IL-1β inhibition alleviates corneal fibrosis. Established corneal scarring models were induced by mechanical injury in WT mice. α-IL-1β antibody (IL-1β neutralizing antibody), anakinra (IL-1R antagonist), or PBS (control group) was subconjunctivally injected. (**A**) Representative bright-field photographs of injured corneas on days 3, 5, and 7 after injury. (**B**) The quantitative statistics of corneal scarring ($n = 10$). (**C**) The representative fluorescent image of α-SMA in corneas at day 7 after injury. Scale bar, 50 μm. (**D**) The qRT-PCR analysis of α-SMA and collagen I mRNA level in corneal tissue on day 7 after injury. (**E**) Western blotting detecting the protein level of α-SMA in corneal tissue on day 7 after injury. All experiments were repeated three times independently. Data are presented as the mean ± standard deviation. $^{*}P < 0.05$, $^{**}P < 0.01$, $^{***}P < 0.001$.

Investigative Ophthalmology & Visual Science

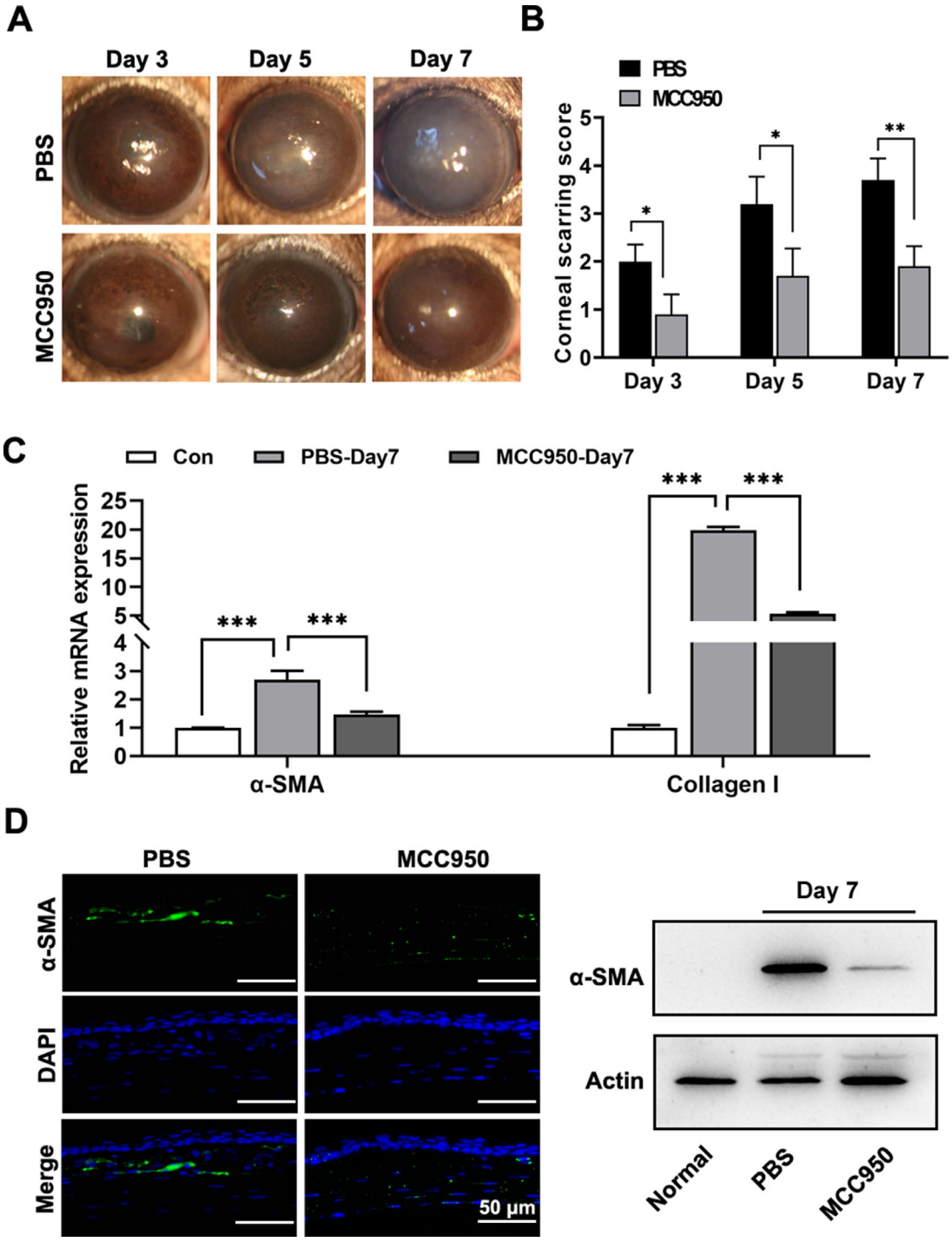

Figure 3. Small inhibitor MCC950 inhibits corneal scar formation. Established corneal scarring models were caused by mechanical injury in WT mice. MCC950 (NLRP3 inhibitor) or PBS (control group) was treated in mice via subconjunctival injection. (**A**) Bright field microscopy of corneas on days 3, 5, and 7 after injury. (**B**) The score of corneal scarring was rated on a scale ($n = 10$). (**C**) Relative mRNA level of fibrotic associated genes (α-SMA, collagen I) in corneal tissue on day 7 after injury. (**D**) Representative fluorescence staining images and relative protein level of α-SMA and in corneas on day 7 after injury. Scale bar, 50 μm. All experiments were repeated three times independently. Data are presented as the mean ± standard deviation. $^{*}P < 0.05$, $^{**}P < 0.01$, $^{***}P < 0.001$.

Macrophage Infiltration Is Associated With Corneal Scarring

To explore the incidence of inflammatory cell, especially macrophage, infiltration during corneal scar formation, single-cell suspensions of corneal tissues were examined using flow cytometry (Fig. 5A). This analysis revealed that the $CD45^{+}$ leukocytes (Fig. 5B) and $CD45^{+}$ $F4/80^{+}$ macrophages (Fig. 5C) increased dramatically in the corneas collected from the WT mice on day 5 after injury. However, the number of $CD45^{+}Ly6G^{+}$ neutrophils was significantly low at the corresponding time points (Fig. 5D).

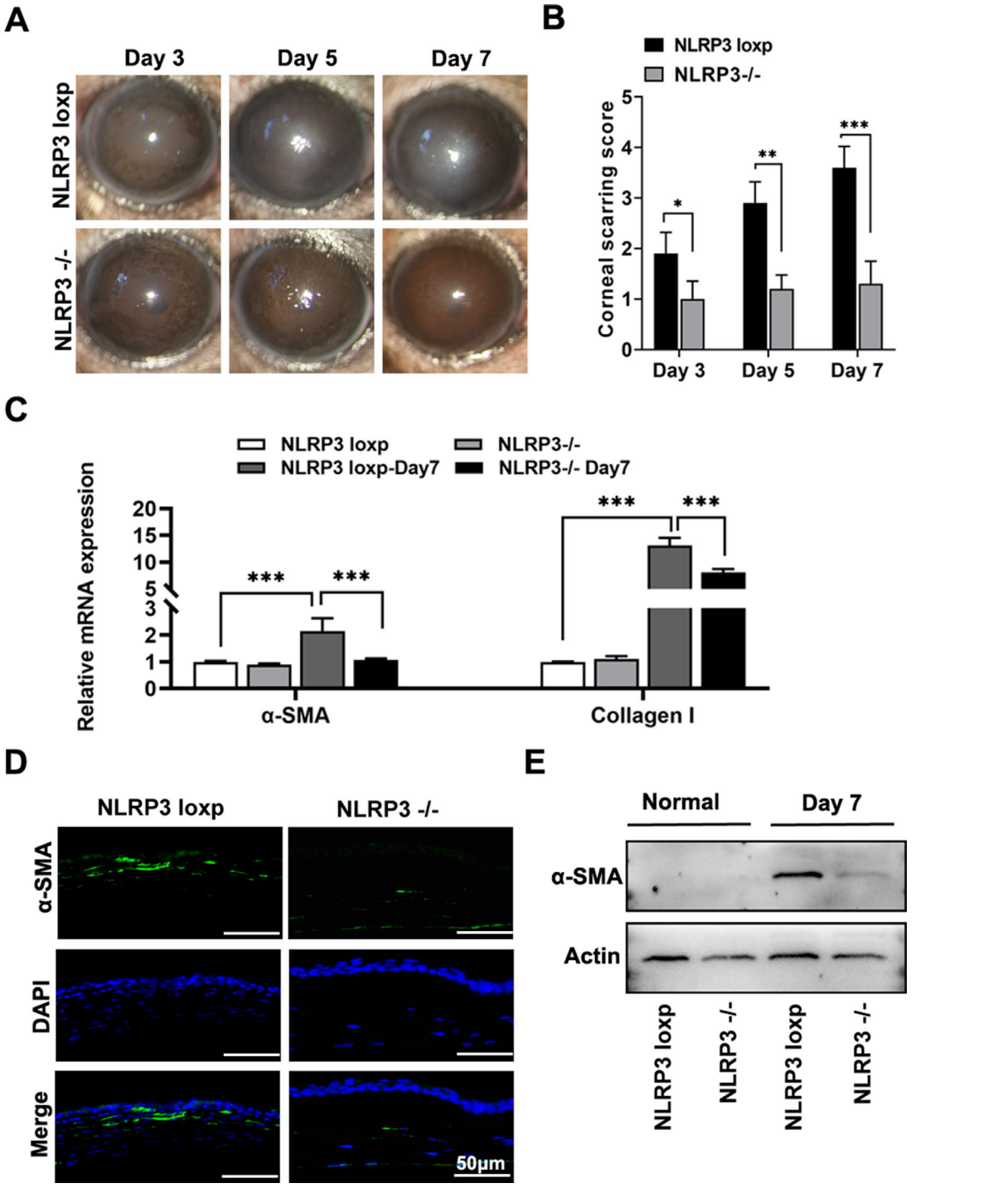

Figure 4. The NLRP3 KO reduces corneal scarring. Mechanical corneal injury was established in *NLRP3*$^{-/-}$ mice and *NLRP3*^{loxp} mice. (**A**) Macroscopic images of corneas under bright field microscopy on days 3, 5, and 7 after wounding. (**B**) The quantitative analysis of corneal scarring ($n = 10$). (**C**) A qRT-PCR analysis for the mRNA expression of fibrosis genes (α-SMA, collagen I) in corneal tissue on day 7 after injury. (**D**) Representative images of fluorescence staining targeting α-SMA in corneas on day 7 after injury. Scale bar, 50 µm. (**E**) The protein level of α-SMA in corneas on day 7 after injury. All experiments were repeated three times independently. Data are presented as the mean ± standard deviation. *$P < 0.05$, **$P < 0.01$, ***$P < 0.001$.

Interestingly, immunofluorescence double staining revealed a strong colocalization of F4/80 with NLRP3 and IL-1β in the corneas of WT mice on day 5 after injury (Fig. 5E). Therefore, macrophage infiltration is closely associated with corneal scar formation.

Macrophage-Specific *NLRP3* KO Reduces Corneal Scarring

Because the NLRP3 inflammasome is highly expressed in tissue macrophages and circulating monocytes, it was vital

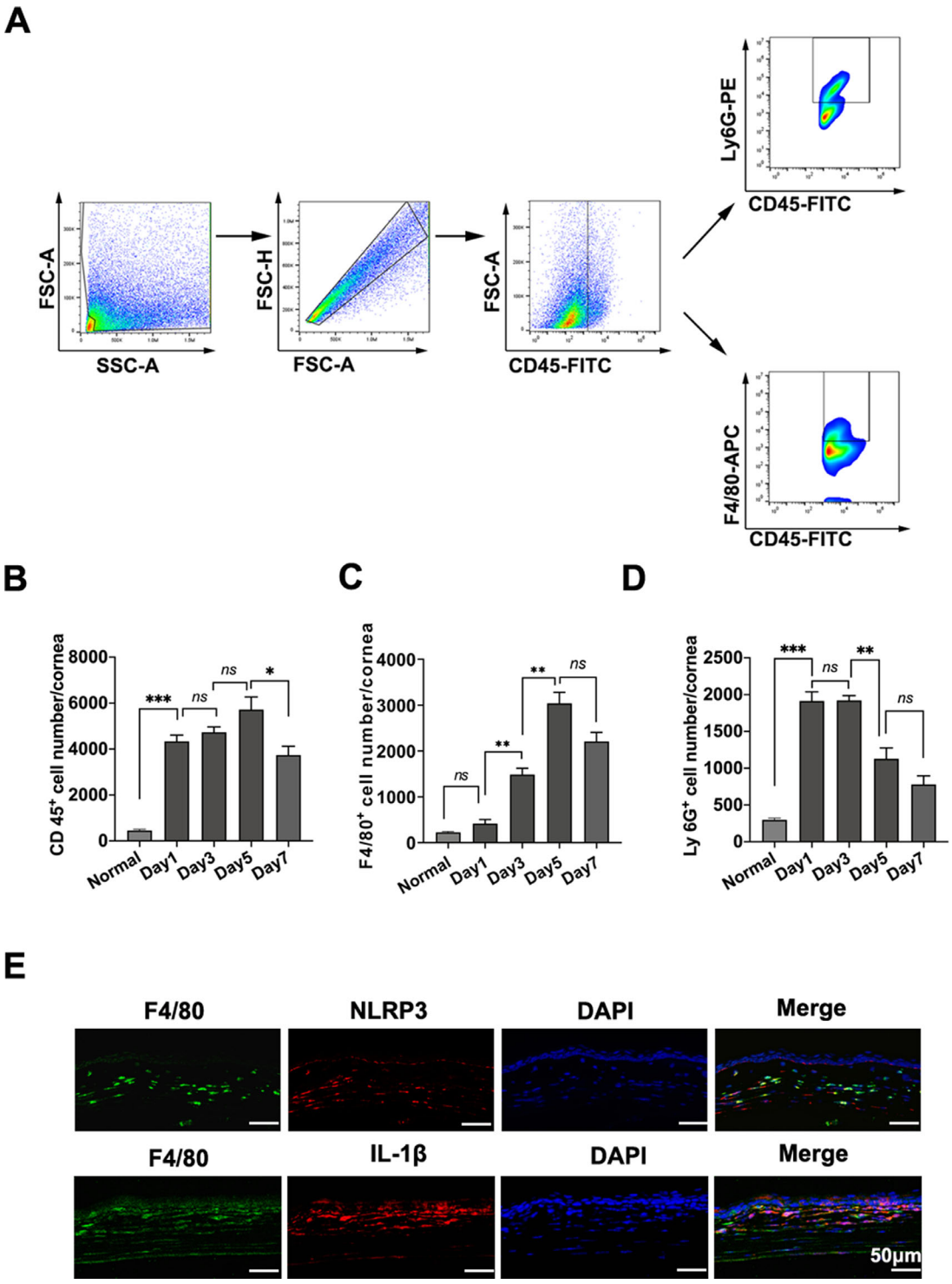

Figure 5. Macrophage infiltration is associated with corneal scar formation. Mechanical injury induced corneal scarring in WT mice and the corneas were removed at different time points. (**A**) Gating strategy for single cells (irregular quadrilateral), blood leukocytes ($CD45^+$, rectangle), neutrophils ($CD45^+/Ly6G^+$, rectangle), macrophages ($CD45^+/F4/80^+$, rectangle). (**B**, **D**) The number of blood cells, neutrophils and macrophages in the normal corneas and corneas on days 1, 3, 5, and 7 after injury ($n = 6$). (**E**) Immunofluorescence staining displayed the colocalization of F4/80 with NLRP3 (top) or IL-1β (bottom) in corneas on day 7 after injury. Scale bar, 50 μm. All experiments were repeated three times independently. Data are presented as the mean ± standard deviation. $^*P < 0.05$, $^{**}P < 0.01$, $^{***}P < 0.001$.

to assess the effect of macrophage-specific *NLRP3* deletion on corneal scarring. Similar to $NLRP3^{-/-}$ mice, the *NLRP3* Lyz-KO mice exhibited a markedly attenuated corneal opacity with a lower scar grade after injury (Figs. 6A and B), as compared with that exhibited by the WT mice. Additionally, these *NLRP3* Lyz-KO mice demonstrated an enhanced ability of corneal epithelial healing on day 3 after injury (Supplementary Fig. S4). Consistent with this finding, the corneas of *NLRP3* Lyz-KO mice exhibit decreased immunostaining of α-SMA, as compared with that in the *Lyz-Cre* mice on day 7

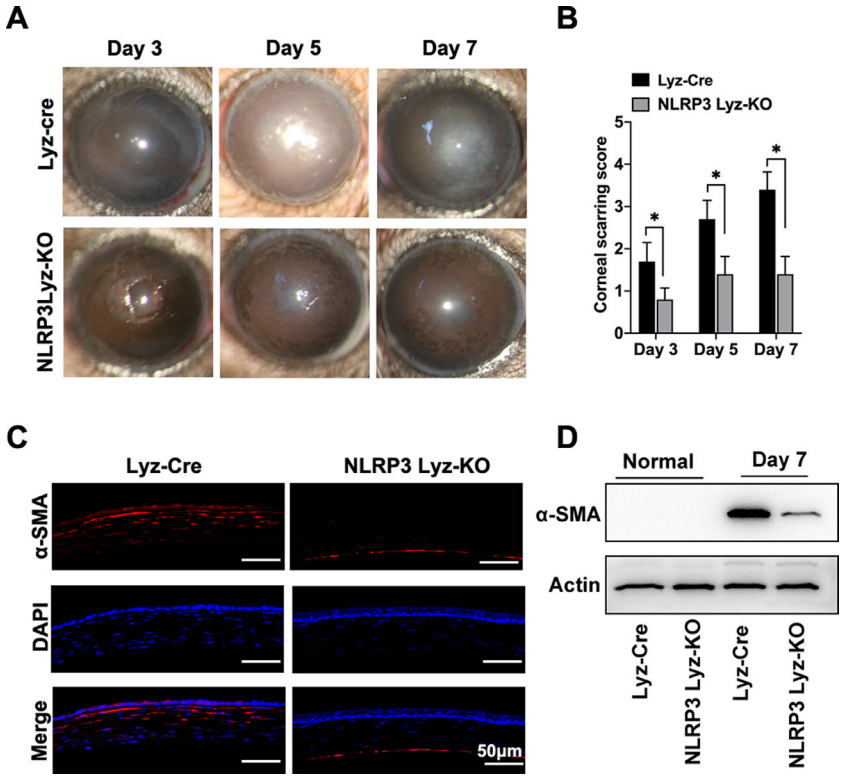

Figure 6. Macrophage-specific NLRP3 KO reduces corneal scarring. Mechanical corneal injury was established in *NLRP3* Lyz-KO (*LyzCre*$^{+}$*NLRP3*$^{loxp/loxp}$) mice and *Lyz-Cre* mice. **(A)** The photograph of corneas under bright field microscope of corneas on days 3, 5, and 7 after injury. (**B**) The quantitative analysis of corneal scarring (n = 10). (**C**) Representative fluorescence staining images showing α-SMA expression in corneas on day 7 after injury. Scale bar, 50 μm. (**D**) The relative protein level of α-SMA in corneas on day 7 after injury. All experiments were repeated three times independently. Data are presented as the mean ± standard deviation. *P < 0.05, **P < 0.01, ***P < 0.001.

after injury (Fig. 6C). In fact, this finding was verified further by the decreased α-SMA protein expression in the *NLRP3* Lyz-KO mice corneas (Fig. 6D), as detected by Western blotting. These observations indicate that macrophage-specific *NLRP3* KO alleviates mechanical damage-induced corneal scarring in vivo.

Corneal Myofibroblast Differentiation Is Mediated by TGF-β1 Secreted by Corneal Epithelial Cells Upon IL-1β Stimulation

TGF-β1 plays a critical role in epithelial migration and corneal scar development. Immunofluorescence staining of the corneal epithelium of WT mice revealed an increase in the TGF-β1 expression in the injured corneas on days 5 and 7 after injury, as compared with that in normal corneas as well as in the injured ones on days 1 and 3 after injury (Fig. 7A). These observations were further confirmed by the progressive increase in the TGF-β1 mRNA (Fig. 7B) and protein expressions (Figs. 7C, D) in the injured corneas of WT mice. In subsequent in vitro experiments, the IL-1β recombinant factor–stimulated human corneal epithelial cells demonstrated an upregulated TGF-β1 mRNA and protein level, as compared with that in the control group; in fact, the TGF-β1 expression increased along with the increase in the dose of IL-1β factor treatment (Figs. 7E–G). Furthermore, the experiments demonstrated that the fluorescence intensity as well as the protein expression level of TGF-β1 was significantly decreased in the corneas of *NLRP3*$^{-/-}$ mice and *NLRP3* Lyz-KO mice, as compared with those in *NLRP3*^{loxp} mice after injury (Figs. 8A–C). To ascertain the effect of NLRP3 activation in macrophages in vitro, peritoneal macrophages were extracted from WT and *NLRP3*$^{-/-}$ mice. Coincidentally, LPS treatment followed by Nig stimulation significantly increased the protein expression of NLRP3 in macrophages derived from WT mice. However, macrophages derived from *NLRP3*$^{-/-}$ mice hardly expressed NLRP3 under similar stimulus (Fig. 8D). Additionally, the NLRP3-induced IL-1β secretion was predominantly decreased in the cell supernatants derived from *NLRP3*$^{-/-}$ mice (Fig. 8E). To examine whether the NLRP3-induced IL-1β secretion by the mouse macrophages has any effect on TGF-β1 expression in the corneal epithelium, the pMCECs derived from the WT mice were preincubated with mouse macrophage supernatants for 24 hours. Even though significantly high TGF-β1 levels were observed in the culture supernatants of LPS-treated macrophages derived from WT mice, this effect was significantly diminished in case of the pMCECs cocultured with supernatants obtained from *NLRP3*$^{-/-}$ macrophages (Fig. 8F). Interestingly, IL-1β–blocking antibodies reversed the IL-1β-induced TGF-β1 upregulation in macrophages from WT mice (Fig. 8G). The macrophage NLRP3-mediated IL-1β production stimulated TGF-β1 expression in the corneal epithelium, thereby causing myofibroblast differentiation.

Investigative Ophthalmology & Visual Science

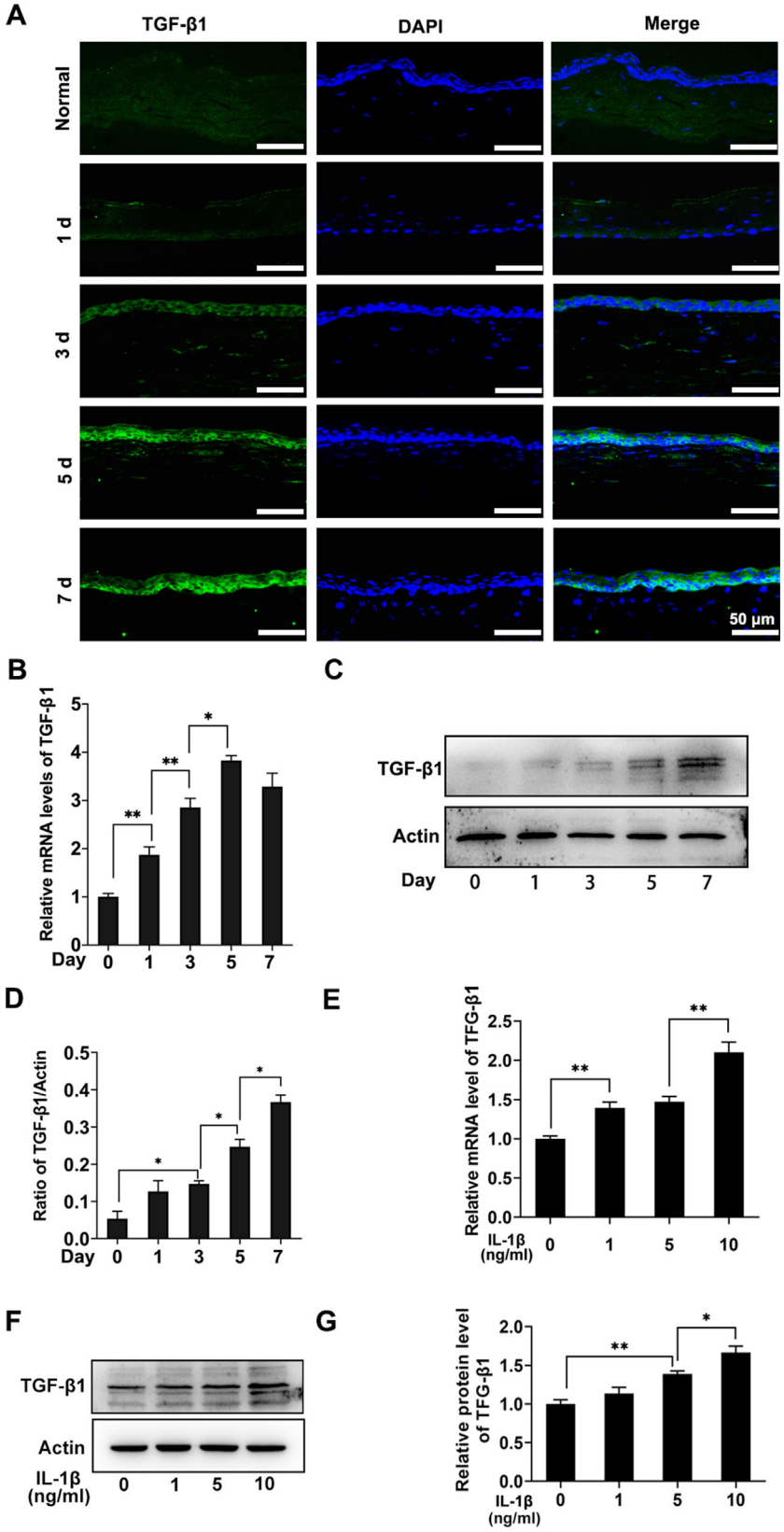

Figure 7. IL-1β stimulates TGF-β1 expression in corneal epithelium. For the in vivo experiment, the corneal tissue was taken from normal WT mice (control group) and WT mice on days 1, 3, 5, and 7 after injury. For the in vitro experiments, IL-1β factor (0, 1, 5, and 10 ng/mL) were added in culture medium of human corneal epithelial cell (HCECs) for 24 hours, the cell samples were collected for qRT-PCR and Western blot. (**A**) Representative photographs of immunofluorescent staining targeting TGF-β1 in corneal tissue. Scale bar, 50 µm. (**B**) qRT-PCR analysis detecting the mRNA level of TGF-β1. (**C**, **D**) Western blotting analysis detecting the protein level of TGF-β1 in corneas. (**E**) The expression of TGF-β1 at mRNA level in HCECs. (F, **G**) Western blot analysis showing TGF-β1 level in HCECs. All experiments were repeated three times independently. Data are presented as the mean ± standard deviation. *$P < 0.05$, **$P < 0.01$, ***$P < 0.001$.

Investigative Ophthalmology & Visual Science

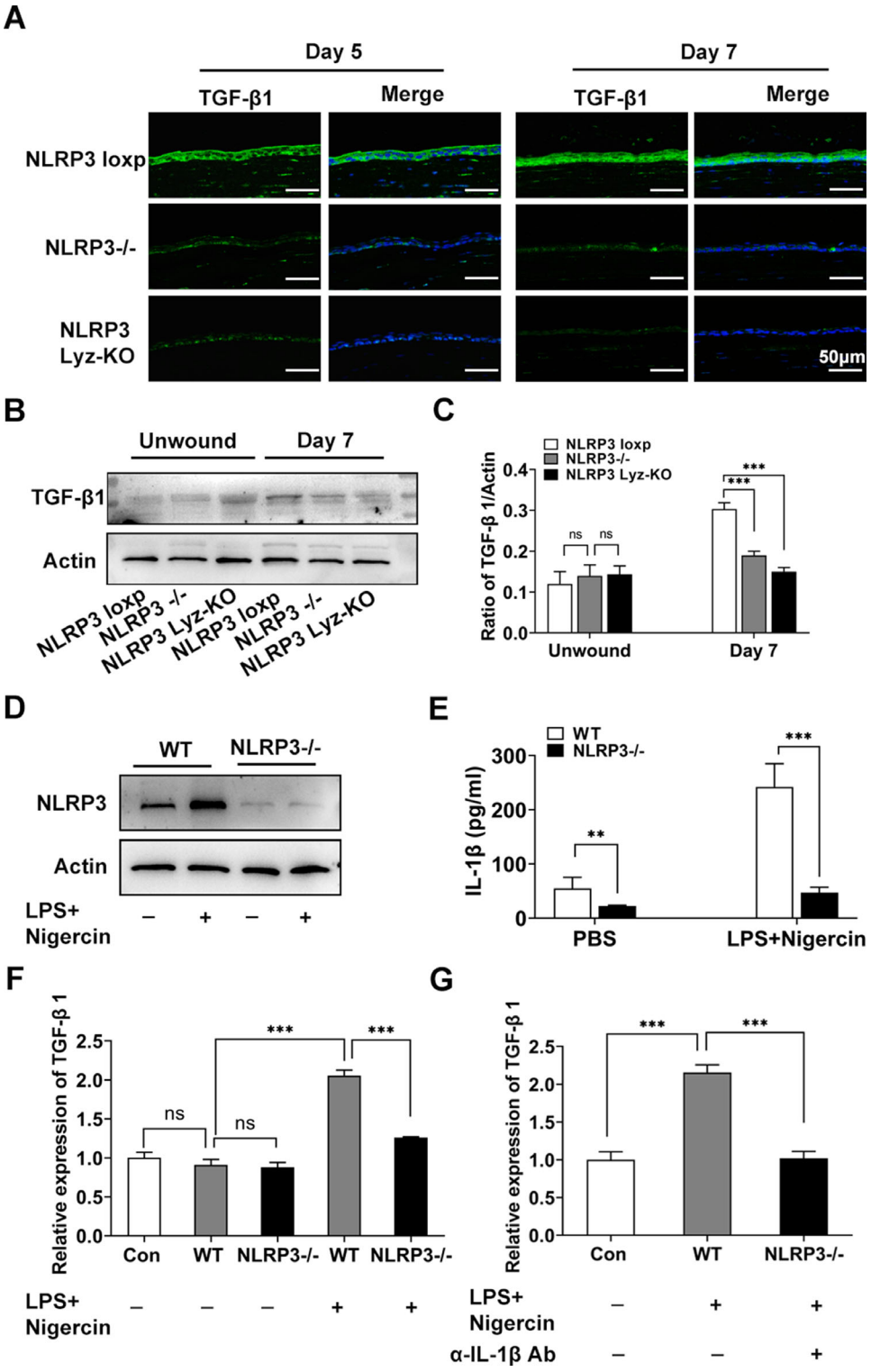

Figure 8. The NLRP3 KO blocks TGF-β1 synthesis in corneal epithelial cells. In vivo, mechanical corneal injury was established in *NLRP3*^{loxp} (control group), *NLRP3*$^{-/-}$ and *NLRP3* Lyz-KO mice respectively. In vitro, peritoneal macrophage extracted from WT mice and *NLRP3*$^{-/-}$ mice. Macrophages were treated with or without LPS and Nigercin (classic NLRP3 inflammasome inducer). Cell precipitation and culture supernatant was collected. Cell supernatant from peritoneal macrophage was cocultured with human corneal epithelial cell (HCECs). (**A**) Representative images of immunofluorescent staining targeting TGF-β1 in corneal tissue post injury. Scale bar, 50 µm. (**B**, **C**) Western blotting analysis comparing protein levels of TGF-β1 between unwound corneas and injured corneas on day 7. (**D**) The protein level of NLRP3 in peritoneal macrophage with or without stimulation. (**E**) Quantitative assay detecting release of IL-1β in cellular supernatant after stimulation with PBS (control group) or LPS with Nigercin (LPS + Nigercin). (**F**) qRT-PCR assay showing TGF-β1 mRNA level in HCECs with or without the macrophage (derived from WT mice and *NLRP3*$^{-/-}$ mice) supernatants. (**G**) The mRNA level of TGF-β1 in HCECs with or without macrophage (derived from WT mice) supernatants. Cell supernatants were exposed to LPS + Nigercin or LPS + Nigercin +_α-IL-1β antibody (IL-1β neutralizing antibody). All experiments were repeated three times independently. Data are presented as the mean ± standard deviation. *$P < 0.05$, **$P < 0.01$, ***$P < 0.001$.

Investigative Ophthalmology & Visual Science

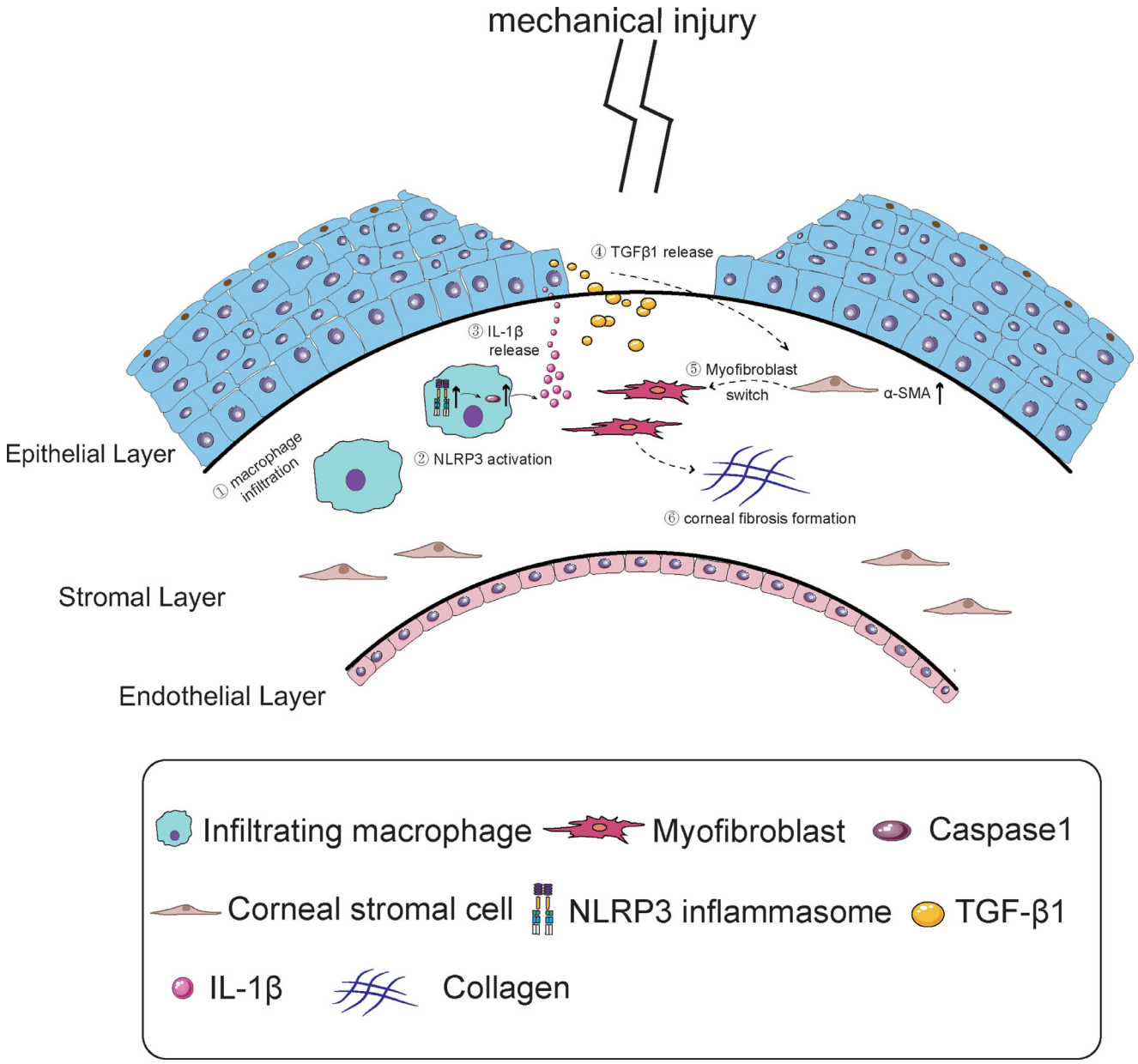

Figure 9. Schematic diagram showing the NLRP3 activation in infiltrating macrophages contributes to corneal fibrosis by inducing TGF-β1 expression in the corneal epithelium.

Discussion

Corneal scarring or corneal fibrosis is characterized by myofibroblast differentiation and a massive amount of extracellular matrix production. The fibroblasts and myofibroblasts establish fibrous connections among the corneal tissues, resulting in a loss of corneal transparency and formation of a corneal scar.[28] This study has confirmed the involvement of the NLRP3/IL-1β signaling pathway of macrophages in corneal scarring and associated inflammatory responses via the regulation of the downstream TGF-β1 (Fig. 9). Moreover, it has been established that blocking the NLRP3/IL-1β signaling pathway inhibits the differentiation of myofibroblasts and maintains corneal transparency.

Emerging evidence has demonstrated that the activation of the NLRP3 inflammasome involves an inflammatory response, which is mainly driven by the release of proinflammatory cytokine IL-1β and IL-18.[29,30] Coincidentally, IL-1β plays a pivotal role in the pathogenesis of inflammation and fibrosis[31,32]; moreover, it amplifies the effects of other cytokines.[18] In liver diseases, the NLRP3 inflammasome activation indirectly induces liver inflammation and fibrosis in a cytokine-dependent manner.[33] In contrast, activation of the inflammasome in hepatic stellate cells directly promotes liver fibrosis.[34] The NLRP3 inflammasome also plays a pivotal role in cardiac fibroblast differentiation, and it mediates the Smad2/3 signaling, thereby resulting in cardiac fibrosis.[35] Additionally, it is involved in the development of pulmonary[36] or renal fibrosis.[37] However, the role of NLRP3 inflammasome in corneal fibrosis has not been explored extensively. Previous studies have demonstrated the proinflammatory role of the NLRP3 inflammasome

Investigative Ophthalmology & Visual Science

in a corneal alkali burn injury model.[38,39] Consistent with this finding, the present study revealed that the NLRP3 inflammasome and its downstream components, namely, ASC, caspase 1, and IL-1β, were significantly elevated during corneal scarring, whereas the *NLRP3*$^{-/-}$ mice exhibited significantly decreased corneal scarring symptoms, including improved corneal transparency and an accelerated healing rate of corneal wounds. Similarly, subconjunctival injection of NLRP3 inhibitor, IL-1β neutralizing antibodies or IL-1R antagonists in WT mice had the same effects in vivo.

Furthermore, the NLRP3 inflammasome is recognized as a crucial complex in the regulation of macrophage function in response to inflammatory stimuli. Coincidentally, fibrosis and scarring occur when a prolonged inflammatory response leads to delayed wound healing.[40] As portrayed in Figure 5D, in the early stages of corneal scarring, the number of neutrophils is significantly upregulated, thereby suggesting that neutrophil infiltration is the first step of corneal fibrosis. Interestingly, as the corneal scarring progressed, that is, on days 5 and 7 after injury, the number of neutrophils decreased, whereas the macrophage recruitment increased. Additionally, the macrophage recruitment process was consistent with the increased expression of NLRP3 during the development of corneal scars. These observations indicate that, after an injury, the NLRP3 in macrophages mediates inflammatory responses in the corneal tissues, ultimately leading to abnormal extracellular matrix deposition and poor remodeling of the corneal stroma. Nonetheless, our preliminary results revealed that the supernatant of NLRP3 activated macrophage did not alter the phenotype of corneal keratocyte (data not shown), indicating that macrophage NLRP3 activation play an indirect role in myofibroblast differentiation.

Recent studies provide increasing evidence indicating that the enhanced TGF-β1 synthesis after a corneal injury is closely associated with the progression of ocular fibrosis.[41–43] Moreover, TGF-β1 and its receptors can inhibit the proliferation of corneal epithelial cells and stimulate the proliferation of mesenchymal fibroblasts.[44–46] Therefore, the increased synthesis of TGF-β1 at the injury site leads to increased myofibroblast differentiation,[47] delayed re-epithelialization,[48,49] and increased collagen gel contraction.[50,51] Interestingly, this study has demonstrated an increase in the TGF-β1 synthesis in the corneal epithelium during the development of corneal scars (Figs. 8A–C). Moreover, in vitro experiments have revealed that NLRP3 activation produces a large amount of IL-1β that, in turn, stimulates TGF-β1 upregulation in the corneal epithelium. Additionally, this effect has been reversed in *NLRP3* KO mice or by the administration of an IL-1β neutralization antibody. Therefore, these experiments have confirmed the role of proinflammatory factor IL-1β in stimulating TGF-β1 synthesis in corneal epithelium post corneal injury, ultimately activating corneal stromal cells and promoting the differentiation of myofibroblasts.

In summary, this study has demonstrated that NLRP3 activation in macrophages mediates a massive release of IL-1β that stimulates TGF-β1 synthesis in the corneal epithelium that, in turn, promotes corneal scar formation. Consequently, the NLRP3/IL-1β signaling pathway might form a promising target for developing a novel, antifibrotic treatment strategy for corneal scarring.

Acknowledgments

The authors thank Editage.com for linguistic assistance during the preparation of this article.

Supported by National Key R&D Program of China Grants (2018YFA0109800), National Natural Science Foundation of China grant (81970782) and China Postdoctoral Science Foundation (No.2019M652328).

Disclosure: **J. Xu**, None; **P. Chen**, None; **X. Luan**, None; **X. Yuan**, None; **S. Wei**, None; **Y. Li**, None; **C. Guo**, None; **X. Wu**, None; **G. Di**, None

References

1. Barrientez B, Nicholas SE, Whelchel A, Sharif R, Hjortdal J, Karamichos D. Corneal injury: clinical and molecular aspects. *Exp Eye Res*. 2019;186:107709.
2. Karamichos D, Guo XQ, Hutcheon AE, Zieske JD. Human corneal fibrosis: an in vitro model. *Invest Ophthalmol Vis Sci*. 2010;51:1382–1388.
3. Mantovani A, Biswas SK, Galdiero MR, Sica A, Locati M. Macrophage plasticity and polarization in tissue repair and remodelling. *J Pathol*. 2013;229:176–185.
4. Dupps WJ, Jr., Wilson SE. Biomechanics and wound healing in the cornea. *Exp Eye Res*. 2006;83:709–720.
5. Li J, Chen J, Kirsner R. Pathophysiology of acute wound healing. *Clin Dermatol*. 2007;25:9–18.
6. Lucas T, Waisman A, Ranjan R, et al. Differential roles of macrophages in diverse phases of skin repair. *J Immunol*. 2010;184:3964–3977.
7. Mahdavian Delavary B, van der Veer WM, van Egmond M, Niessen FB, Beelen RH. Macrophages in skin injury and repair. *Immunobiology*. 2011;216:753–762.
8. Ploeger DT, Hosper NA, Schipper M, Koerts JA, de Rond S, Bank RA. Cell plasticity in wound healing: paracrine factors of M1/M2 polarized macrophages influence the phenotypical state of dermal fibroblasts. *Cell Commun Signal*. 2013;11:29.
9. Li S, Li B, Jiang H, et al. Macrophage depletion impairs corneal wound healing after autologous transplantation in mice. *PloS One*. 2013;8:e61799.
10. Wynn TA, Ramalingam TR. Mechanisms of fibrosis: therapeutic translation for fibrotic disease. *Nat Med*. 2012;18:1028–1040.
11. He L, Marneros AG. Macrophages are essential for the early wound healing response and the formation of a fibrovascular scar. *Am J Pathol*. 2013;182:2407–2417.
12. Pesce JT, Ramalingam TR, Mentink-Kane MM, et al. Arginase-1-expressing macrophages suppress Th2 cytokine-driven inflammation and fibrosis. *PLoS Pathog*. 2009;5:e1000371.
13. Korns D, Frasch SC, Fernandez-Boyanapalli R, Henson PM, Bratton DL. Modulation of macrophage efferocytosis in inflammation. *Front Immunol*. 2011;2:57.
14. Zhang J, Liu X, Wan C, et al. NLRP3 inflammasome mediates M1 macrophage polarization and IL-1beta production in inflammatory root resorption. *J Clin Periodontol*. 2020;47:451–460.
15. Trachalaki A, Tsitoura E, Mastrodimou S, et al. Enhanced IL-1β release following NLRP3 and AIM2 inflammasome stimulation is linked to mtROS in airway macrophages in pulmonary fibrosis. *Front Immunol*. 2021;12:661811.
16. Amselem S, de Boysson H, Aouba A, et al. Brucella abortus infection elicited hepatic stellate cell-mediated fibrosis through inflammasome-dependent IL-1β production. *Liver Int*. 2019;10:3036.

17. Krishnan SM, Ling YH, Huuskes BM, et al. Pharmacological inhibition of the NLRP3 inflammasome reduces blood pressure, renal damage, and dysfunction in salt-sensitive hypertension. *Cardiovasc Res*. 2019;115:776–787.
18. Dong M, Yang L, Qu M, et al. Autocrine IL-1beta mediates the promotion of corneal neovascularization by senescent fibroblasts. *Am J Physiol Cell Physiol*. 2018;315:C734–C743.
19. Wang X, Qu M, Li J, Danielson P, Yang L, Zhou Q. Induction of fibroblast senescence during mouse corneal wound healing. *Invest Ophthalmol Vis Sci*. 2019;60:3669–3679.
20. Mittal SK, Omoto M, Amouzegar A, et al. Restoration of corneal transparency by mesenchymal stem cells. *Stem Cell Rep*. 2016;7:583–590.
21. Qu M, Zhang X, Hu X, et al. BRD4 inhibitor JQ1 inhibits and reverses mechanical injury-induced corneal scarring. *Cell Death Discov*. 2018;4:5.
22. Sharma A, Mehan MM, Sinha S, Cowden JW, Mohan RR. Trichostatin a inhibits corneal haze in vitro and in vivo. *Invest Ophthalmol Vis Sci*. 2009;50:2695–2701.
23. Tanei T, Leonard F, Liu X, et al. Redirecting transport of nanoparticle albumin-bound paclitaxel to macrophages enhances therapeutic efficacy against liver metastases. *Cancer Res*. 2016;76:429–439.
24. Yu C, Chen P, Xu J, et al. hADSCs derived extracellular vesicles inhibit NLRP3inflammasome activation and dry eye. *Sci Rep*. 2020;10:14521.
25. Liu Y, Di G, Wang Y, Chong D, Cao X, Chen P. Aquaporin 5 facilitates corneal epithelial wound healing and nerve regeneration by reactivating Akt signaling pathway. *Am J Pathol*. 2021;191:1974–1985.
26. Xu J, Chen P, Zhao G, et al. Copolymer micelle-administered melatonin ameliorates hyperosmolarity-induced ocular surface damage through regulating PINK1 mediated mitophagy. *Curr Eye Res*. 2022;47:688–703.
27. Tahvildari M, Omoto M, Chen Y, et al. In vivo expansion of regulatory T cells by low-dose interleukin-2 treatment increases allograft survival in corneal transplantation. *Transplantation*. 2016;100:525–532.
28. de Oliveira RC, Wilson SE.Fibrocytes, wound healing, and corneal fibrosis. *Invest Ophthalmol Vis Sci*. 2020;61:28.
29. Cordero MD, Alcocer-Gomez E, Ryffel B. Gain of function mutation and inflammasome driven diseases in human and mouse models. *J Autoimmunity*. 2018;91:13–22.
30. Strowig T, Henao-Mejia J, Elinav E, Flavell R. Inflammasomes in health and disease. *Nature*. 2012;481:278–286.
31. Wilson SE. Interleukin-1 and transforming growth factor beta: commonly opposing, but sometimes supporting, master regulators of the corneal wound healing response to injury. *Invest Ophthalmol Vis Sci*. 2021;62:8.
32. Wilson SE, Esposito A. Focus on molecules: interleukin-1: a master regulator of the corneal response to injury. *Exp Eye Res*. 2009;89:124–125.
33. Ning ZW, Luo XY, Wang GZ, et al. MicroRNA-21 mediates angiotensin II-induced liver fibrosis by activating NLRP3 inflammasome/IL-1beta axis via targeting Smad7 and Spry1. *Antioxid Redox Signal*. 2017;27:1–20.
34. Kang LL, Zhang DM, Ma CH, et al. Cinnamaldehyde and allopurinol reduce fructose-induced cardiac inflammation and fibrosis by attenuating CD36-mediated TLR4/6-IRAK4/1 signaling to suppress NLRP3 inflammasome activation. *Sci Rep*. 2016;6:27460.
35. Bracey NA, Gershkovich B, Chun J, et al. Mitochondrial NLRP3 protein induces reactive oxygen species to promote Smad protein signaling and fibrosis independent from the inflammasome. *J Biol Chem*. 2014;289:19571–19584.
36. Song C, He L, Zhang J, et al. Fluorofenidone attenuates pulmonary inflammation and fibrosis via inhibiting the activation of NALP3 inflammasome and IL-1beta/IL-1R1/MyD88/NF-kappaB pathway. *J Cell Mol Med*. 2016;20:2064–2077.
37. Chi HH, Hua KF, Lin YC, et al. IL-36 signaling facilitates activation of the NLRP3 inflammasome and IL-23/IL-17 axis in renal inflammation and fibrosis. *J Am Soc Nephrol*. 2017;28:2022–2037.
38. Bian F, Xiao Y, Zaheer M, et al. Inhibition of NLRP3 inflammasome pathway by butyrate improves corneal wound healing in corneal alkali burn. *Int J Mol Sci*. 2017;18:562.
39. Shimizu H, Sakimoto T, Yamagami S. Pro-inflammatory role of NLRP3 inflammasome in experimental sterile corneal inflammation. *Sci Rep*. 2019;9:9596.
40. Landen NX, Li D, Stahle M. Transition from inflammation to proliferation: a critical step during wound healing. *Cell Mol Life Sci*. 2016;73:3861–3885.
41. Yeung V, Sriram S, Tran JA, et al. FAK inhibition attenuates corneal fibroblast differentiation in vitro. *Biomolecules*. 2021;11:1682.
42. Stahnke T, Kowtharapu BS, Stachs O, et al. Suppression of TGF-beta pathway by pirfenidone decreases extracellular matrix deposition in ocular fibroblasts in vitro. *PloS One*. 2017;12:e0172592.
43. Wilson SE, Sampaio LP, Shiju TM, Hilgert GSL, de Oliveira RC. Corneal opacity: cell biological determinants of the transition from transparency to transient haze to scarring fibrosis, and resolution, after injury. *Invest Ophthalmol Vis Sci*. 2022;63:22.
44. Chen Q, He G, Zhang W, et al. Stromal fibroblasts derived from mammary gland of bovine with mastitis display inflammation-specific changes. *Sci Rep*. 2016;6:27462.
45. Cui HS, Hong AR, Kim JB, et al. Extracorporeal shock wave therapy alters the expression of fibrosis-related molecules in fibroblast derived from human hypertrophic scar. *Int J Mol Sci*. 2018;19:124.
46. Haber M, Cao Z, Panjwani N, Bedenice D, Li WW, Provost PJ. Effects of growth factors (EGF, PDGF-BB and TGF-beta 1) on cultured equine epithelial cells and keratocytes: implications for wound healing. *Vet Ophthalmol*. 2003;6:211–217.
47. Carrington LM, Albon J, Anderson I, Kamma C, Boulton M. Differential regulation of key stages in early corneal wound healing by TGF-beta isoforms and their inhibitors. *Invest Ophthalmol Vis Sci*. 2006;47:1886–1894.
48. Nuwormegbe SA, Kim SW. AMPK activation by 5-amino-4-imidazole carboxamide riboside-1-beta-D-ribofuranoside attenuates alkali injury-induced corneal fibrosis. *Invest Ophthalmol Vis Sci*. 2020;61:43.
49. Sommer K, Sander AL, Albig M, et al. Delayed wound repair in sepsis is associated with reduced local pro-inflammatory cytokine expression. *PloS One*. 2013;8:e73992.
50. Lygoe KA, Wall I, Stephens P, Lewis MP. Role of vitronectin and fibronectin receptors in oral mucosal and dermal myofibroblast differentiation. *Biol Cell*. 2007;99:601–614.
51. Maruri DP, Miron-Mendoza M, Kivanany PB, et al. ECM stiffness controls the activation and contractility of corneal keratocytes in response to TGF-beta1. *Biophys J*. 2020;119:1865–1877.

Investigative Ophthalmology & Visual Science